

Experimental study of friction in pneumatic seals

Abdelhak AZZI^{a,b,*}, Abdelghani MAOUI^a, Aurelian FATU^b, Sebastien FILY^a, Dominique SOUCHET^b,

^aCETIM Pôle Technologie de l'Étanchéité 74, route de la Jonelière – BP 82617, 44326, Nantes, France

^bDépartement Génie Mécanique et Système Complexes, Institut Pprime, CNRS-Université de Poitiers-ISAE-ENSMA, UPR 3346, 86962 Futuroscope Chassenuil, France.

*Corresponding author: abdelhak.azzi@univ-poitiers.fr

Abstract

Friction in the pneumatic cylinders is one of the most important factors impacting their performances and their reliability.

This paper proposes to experimentally study the influence of the different seal geometry used in pneumatic cylinders and the operating conditions on the friction behavior.

Experimental tests are conducted on industrial commercial pneumatic cylinders. In addition, piston and rod seals are tested separately to study the friction caused by each seal.

The results show that the effect of pneumatic pressure on the friction is greater than that of the velocity. The seal geometry has a significant effect on friction, which is magnified as the seal diameter increases. In addition, 90% of the friction in pneumatic cylinders is due to the piston seals.

KEYWORDS

Friction force, Pneumatic cylinders, Dynamic seals.

1. Introduction

Pneumatic cylinders are used in many industrial applications to produce forces in reciprocating linear motion. Compared to other devices producing the same forces, such as hydraulic cylinders, pneumatic cylinders have advantages that include high speed, reliability, low cost, easy assembly, easy maintenance and availability of compressed air in almost all industrial installations. These advantages make the pneumatic cylinders competitive in many engineering applications.

The sealing solution in pneumatic cylinders is of major importance because it allows to maintain the cylinder pneumatic power and contribute to the amount of the energy dissipated by friction. It has also a direct impact on the lifetime of the pneumatic cylinders.

A seal malfunction, caused by a wrong choice of the seal material or geometry, on unsuitable surface texture, an incompatible lubricant or other inappropriate tribological factors, results to high friction, low sealing performance, and low system efficiency.

A thorough knowledge of the friction force of pneumatic seals depending on the operating conditions is an important step in optimizing seal performances and defining better preventive maintenance procedures of pneumatic cylinders [1]. This

helps to improve the performance and the efficiency of pneumatic components in order to extend their service life and have a wide range of industrial applications that comply with increasingly restrictive pollution legislation.

Experimental and numerical investigations presented in international literature [2-8] have demonstrated the importance of measuring the friction force of pneumatic and hydraulic cylinders as accurately as possible, taking into account all the physical factors such as velocity, pressure [2-5] or other tribological factors [8].

Raparelli et al. [2] experimentally validated a numerical approach to evaluate the seals performances, under different pressure and velocity conditions, under both dry and boundary lubrication conditions. The numerical approach is obtained by an iterative process which uses the experimental friction coefficient measured as a function of velocity and lubrication conditions. Results show a good agreement between the experimental results and the numerical simulations. Moreover, it has been shown that the friction force increases with velocity and pressure.

Belforte et al [3] developed a specific device to measure the friction forces in pneumatic cylinders of different sizes and for a wide range of velocities and pressures. The experimental results show that the friction force increases with the velocity. Moreover, the influence of pressure is important for high velocities and large diameters. With regard to the effect of diameters, they found that the friction force increases (almost) proportionally with the cylinder diameter.

Belforte et al [4] present a seal development procedure used to design a new seal for spool valves application able to operate in dry condition. Experimental tests and finite element analyses (FEA) were performed to evaluate the performances of the new sealing system under different operating conditions (pressures and velocities) and by taking into account the machining tolerances. Two seal configurations have been designed. When the system is lubricated, no significant differences between the existing commercial seal and the new seals were found. On the contrary, in dry conditions, the new design has lower friction force.

Chang et al [5] studied the effect of dry and lubricated conditions on the friction behavior. They showed that the friction force was significantly reduced by using grease as a lubricant for pneumatic seals.

Belfort et al [6] have designed a test ring able to measure the friction force generated by a single seal but also the overall friction force caused by all the sliding seals in a pneumatic cylinder. Tests were carried out in different operating conditions (velocities and pressures) with similar sealing system characteristics but produced by different manufacturers. The results show the dependence of the friction force on the direction of stroke for all the tested seals.

FEA and experimental tests presented in references [7] and [8] led to the development of a new elastomeric seal that improves friction performances. They demonstrated the importance of the seal cross-sectional shape to improve friction performance and sealing efficiency of pneumatic seals.

Studies on failure phenomena occurring in pneumatic components have been carried out and described in references [9] and [10]. These works highlighted the importance of correct grease-lubrication conditions and the seal material properties on wear resistance.

Mazza et al. [11] identified the contribution of each type of seals, rod and piston, to the total friction force of pneumatic cylinders by combining a new analytical approach and experimental measurements. Their analytical model is based on the geometrical and material properties of the seal. It processes separately the friction contribution of each seal, while the experiments provide the friction force of the complete actuator. The proposed model is only validated for certain operating conditions.

In references [12] [13] the authors investigate friction force on commercial pneumatic cylinders by means of special test rigs. This investigation allowed developing new low friction seal geometries and the development of a model for predicting friction in pneumatic cylinders.

To reduce friction and wear of sliding sealing systems, Verheyde et al [14] examined the influence of two different surface treatment techniques applied to an elastomeric. The results in terms of friction reduction seem to be promising.

The aim of the present work is to evaluate the sealing performance of industrial pneumatic cylinders and pneumatic seals under a wide range of operating conditions and seal geometries. In order to achieve this, an experimental device was developed to measure seal performances in terms of friction force. First, the test conditions and measurements obtained on a commercial double-acting pneumatic cylinder are described and commented. Secondly, the friction generated by different seal geometries and cylinder diameters as a function of stroke direction, pneumatic pressure and piston velocity are studied.

2. Test setup and method

2.1. Test equipment

Friction force measurements were performed by means of the test apparatus schematically presented in Figure 1. It contains a control system and a test cell. It allows tests on complete pneumatic cylinders or on a specific test cell. The test cell consists of a cylinder in which a moving piston is housed.

The control system includes an electrical actuator (ETB100M05), which provides the linear motion and an instrumentation system consisting in pressure sensors and proportional valve meant to control the pressure in the cylinder chambers. The tested rod is connected to the electric actuator through a ball joint and a load cell of the type S9M/20kN (having accuracy of 0.02% of the full scale) used to measure the axial force of the pneumatic cylinder. The electric actuator controls the displacement and the velocity of the tested rod.

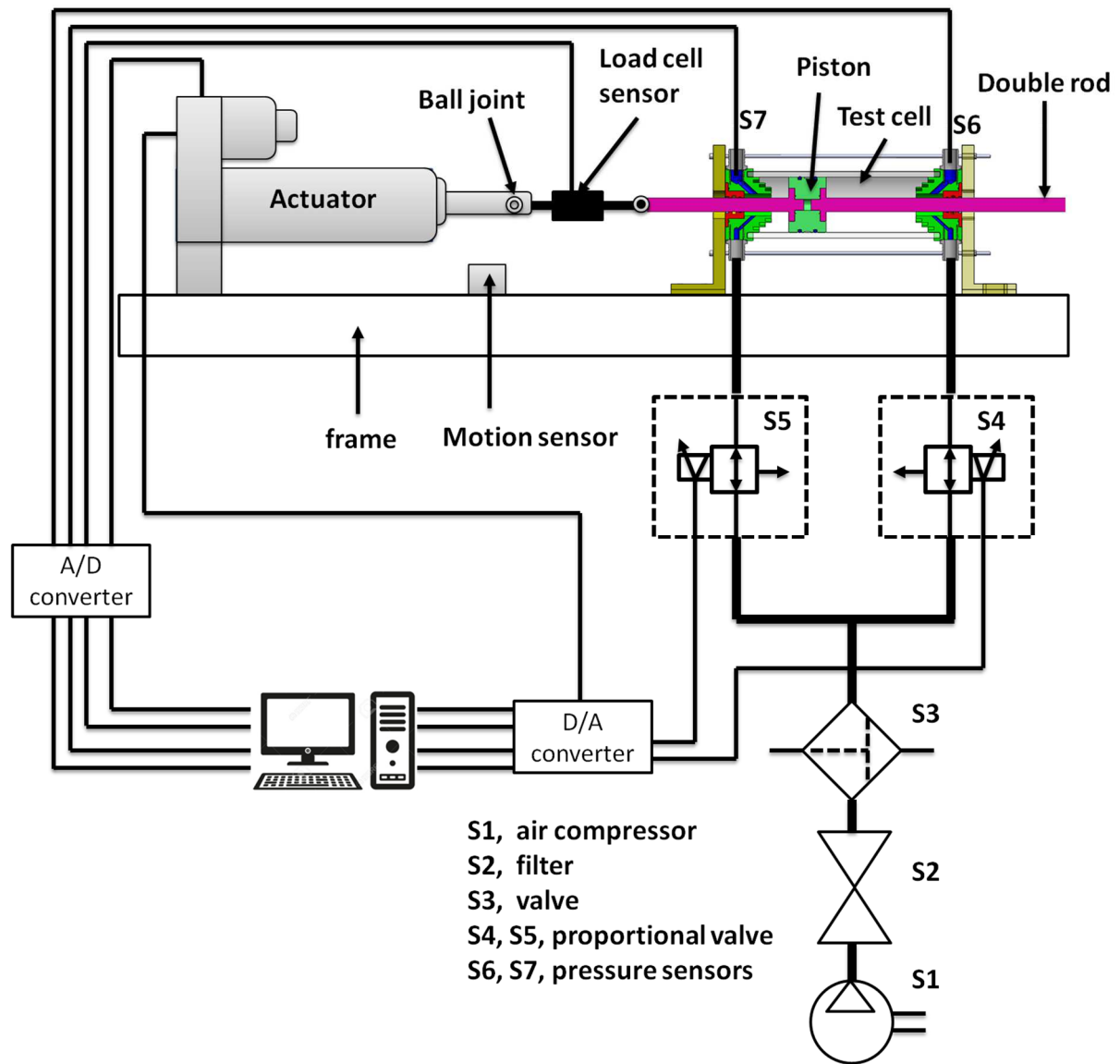



Figure 1: Schematic view of the overall experimental test rig

2.2. Tested seals

Table 1 presents the different tested pneumatic seals. The tested seals are three rod seals and three piston seals. The different seals are designated by seal cross section with a representative letter (U for U-cup, X for X-ring, O for O-ring and RS for Rod-Scraper) followed by a number which corresponds to the diameter of rod or cylinder. The seals materials are designated by PUR for polyurethane and NBR for Nitrile butadiene rubber.

Tested seals	Designation	Material	Hardness (IRHD)	Cross section
	U-100	PUR	80	



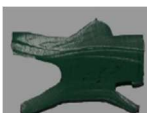


Piston seals	X-100	NBR	65	
	O-100	NBR	70	
Rod seals	RS--25	PUR	90	
	U-25	PUR	90	
	O-25	NBR	78	

Table 1: Definition of tested rod and piston seals

In order to be representative to the actual operating conditions of the pneumatic seals, the mechanical parts (rod, piston, and cylinder) used during the tests are derived from commercial pneumatic cylinders. To recover the various rods, pistons and cylinders required for the tests, the complete cylinders are dismantled. The geometric and material properties of these parts are summarized in Table 2.

	Designation	Material	Diameter (mm)
Piston	Piston 50	polyoxymethylene acetal (POM)	50
	Piston 63		63
	Piston 80		80
	Piston 100	aluminum alloy	100
Rod	Rod 25	chrome steel	25
Cylinder	-	anodized aluminum	50, 63, 80 and 100

Table 2: Rod, piston and cylinder definition

2.3. Friction force

The different forces acting on the cylinder while the piston is moving with a velocity V are presented in Figure 2.

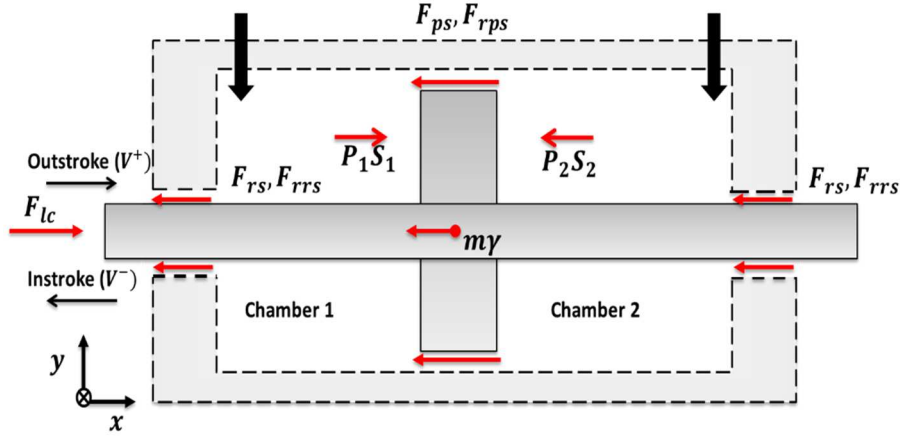


Figure 2: Forces acting in the industrial pneumatic cylinder (configuration 1)

The balance of these forces is given by equations 1.

$$F_{lc} + P_1 S_1 - P_2 S_2 - (F_{rs} + F_{rrs} + F_{ps} + F_{rps}) = m\gamma \quad (1)$$

Where $P_1 S_1$ and $P_2 S_2$ are the air forces acting on the piston in chamber 1 and chamber 2, respectively, with P_1 and P_2 the absolute pressures¹ on the chamber 1 and 2 and S_1 and S_2 the piston surfaces. F_{lc} is the external axial force applied on the rod by the driving actuator, $m\gamma$ the inertial force and F_{rs} , F_{rrs} , F_{ps} , F_{rps} the friction forces.

Assuming that the inertial force is neglected in steady state, the total friction force F_f is given by the sum of the friction forces of the seals and the guiding rings:

$$F_f = F_{lc} + P_1 S_1 - P_2 S_2 \quad (2)$$

The pneumatic cylinder schematic representation from figure 2 corresponds to the first configuration of the test cell i.e. a complete pneumatic cylinder. Figure 3 and 4 show two other different configurations that will be considered in this paper. Configuration 2 is used to measure the friction force generated by a single piston seal. During tests, a pneumatic (air) pressure is applied in chamber 2 when chamber 1 is under atmospheric pressure. Configuration 3 is used to measure the friction force generated by a single rod seal.

¹ all pressure values in this manuscript are absolute pressures

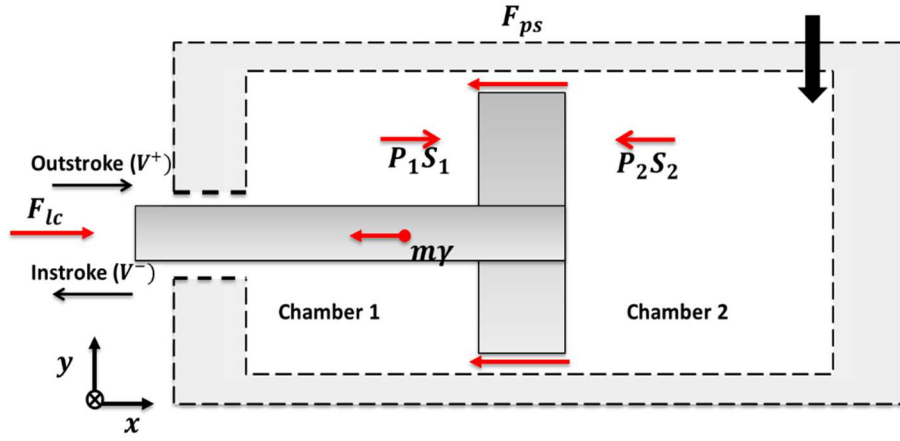


Figure 3: Schematic representation of Configuration 2: single piston seal

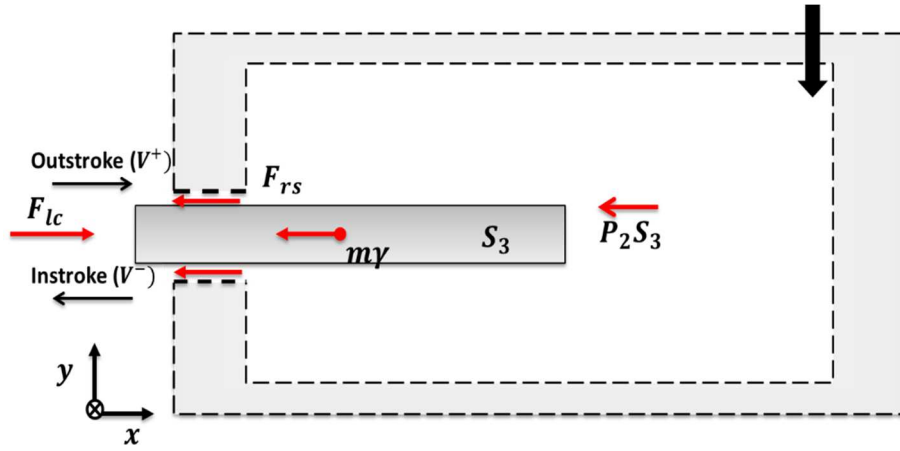


Figure 4: Schematic representation of Configuration 3: single rod seal

2.4. Test conditions

Table 3 presents the operating conditions of the various experimental tests carried out. The tests are performed for different pneumatic cylinder configurations, seals, diameters, air pressures and rod speeds. The three different test cell configurations presented in the previous paragraph are used. Twenty instroke/outstroke cycles are run for each configuration.

Configurations	Tests	Piston (mm)	Rod (mm)	Piston seal	Rod seal	P ₁ (bar)	P ₂ (bar)	Velocity (mm/s)	
								[10,200]	[50,300]
1 Whole cylinder	Test 1	Piston 100	Rod 25	U-100	RS-25	1	[1-10]		X
	Test 2	/	Rod 25	/	RS-25				

2 Piston seals	Test 3	Piston 100	/	U-100	/	1	[1-10]	X
	Test 4	Piston 80	/	U-80	/			
	Test 5	Piston 63	/	U-63	/			
	Test 6	Piston 50	/	U-50	/			
	Test 7	Piston 100	/	X-100	/			
	Test 8	Piston 100	/	O-100	/			
	3 Rod seals	Test 9	/	Rod 25	/			
Test 10		/	Rod 25	/	U-25			
Test 11		/	Rod 25	/	O-25			

Table 3: Tests conditions

The first tests are carried out on a complete double-acting commercial pneumatic cylinder (configuration 1). It has a 100 mm bore, a double rod diameter of 25 mm, a stroke of 500 mm and is grease-lubricated. The cylinder barrel is made of anodized aluminum, the rods of chromed steel and the piston of aluminum alloy. The piston is sealed by two polyurethane lip seals (U-100) and one piston guiding ring. The rod is sealed by two polyurethane rod sealing scrapers (RS-25) with two rod guiding rings mounted in the rod cover. The tests are made at different air pressures within the cylinder chamber 2 (see figure 2) and for both directions of the piston/rod assembly. The velocity varies from 50 mm/s to 300 mm/s. Two configurations of the test cell are investigated.

The first test (Test 1) corresponds to configuration 1, represented in Figure 2. As it will be seen bellow, the friction forces measured for this configuration are comparable to those obtained by Belforte et al. [3] under similar operating conditions.

Test 2 is also performed on the commercial cylinder, but the two piston seals and the piston guiding ring are removed. The purpose is made to evaluate the ratio between the friction generated by the piston seals and that generated by the rod seals.

Tests from 3 to 6 are carried out on U-cup piston seals of for four different diameters (configuration 2 represented in Figure 3). Tests 7 and 8 are also performed for piston seals by considering two different cross

sections (X-100 and O-100 seals). The velocity varies from 10 mm/s to 200 mm/s and the air pressure in chamber 2 ranges between 1 bar and 10 bars.

The last three tests (9 to 11) are performed to evaluate the friction of three different rod seals (configuration 3, represented in Figure 4) for velocities varying from 10 mm/s to 200 mm/s and pressures ranging between 1 bar and 10 bars.

In order to understand the results presented below it is important to specify that, when referring to figure 2, 3 and 4, the velocity is considered positive for a left-to-right movement (outstroke) and negative for a right-to-left movement (instroke). Therefore, in configuration 1 and 2, the chamber 2 behaves as a resistant chamber when the velocity is positive or as a driving chamber when the velocity is negative.

During the tests, three parameters are imposed: the air pressure in the pneumatic chambers, the rod velocity, and the rod axial position. The air pressure inside the cylinder chambers is adjusted by a proportional valve. Figure 5 shows an example of how the speed and position of the rod vary over a typical outstroke/instroke cycle. As we can observe, the two parameters are controlled with good accuracy.

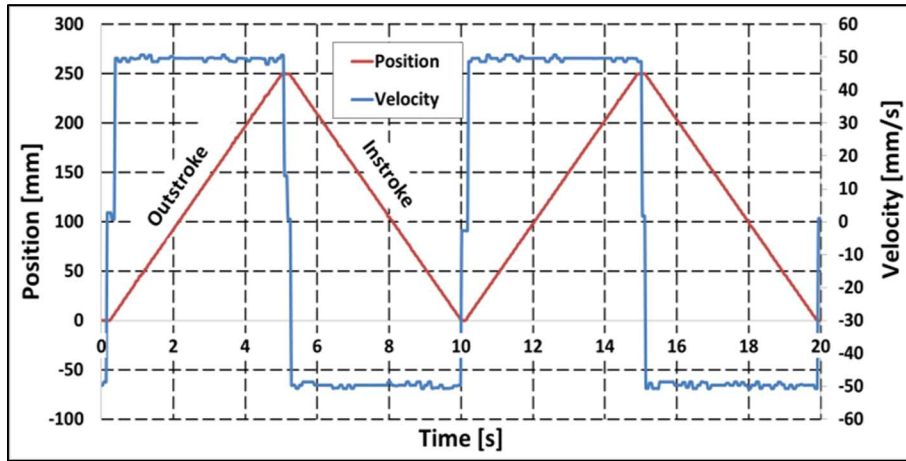


Figure 5: Typical cycle

3. Experimental results

In this section, the experimental results obtained for the various tests performed according to the configurations defined in Table 3 are presented. The friction behavior of the rod and piston seals are presented and analyzed as a function of air pressure, rod velocity, seal design, and seal diameter. The design effect of the seal includes the effect of the seal material and that of the seal cross-section.

3.1. Effect of air pressure

The results presented in this section mainly concern the whole cylinder configuration (Test 1 and Test 2 in Table 3). Figure 6 shows the variation of the measured friction force for two complete outstroke/instroke cycles when $P_1 = P_2 = 1$ bar (atmospheric pressure) and the velocity is 50mm/s. As can be seen, the friction force

recorded during the strokes is stable, which attests to the good accuracy of the measurement. Even if the configuration of the test cell is theoretically perfectly symmetrical, a positive offset (15 N or $\approx 37.5\%$ of the instroke friction force) can be observed between the friction modulus measured during the outstroke and that measured during the instroke. The only explanation of this behavior lies in the manufacturing defects of the commercial cylinder used for this investigation: differences in the geometry of the housing of the various seals can quickly lead to asymmetry during operation. However, it should be mentioned that the 15N offset of the friction force between the two strokes is negligible compared to the forces developed by the cylinder in real applications (for example for a 1 bar difference of pressure between the two chambers, the developed driving force is about 700 to 800 N, as shown in figure 7).

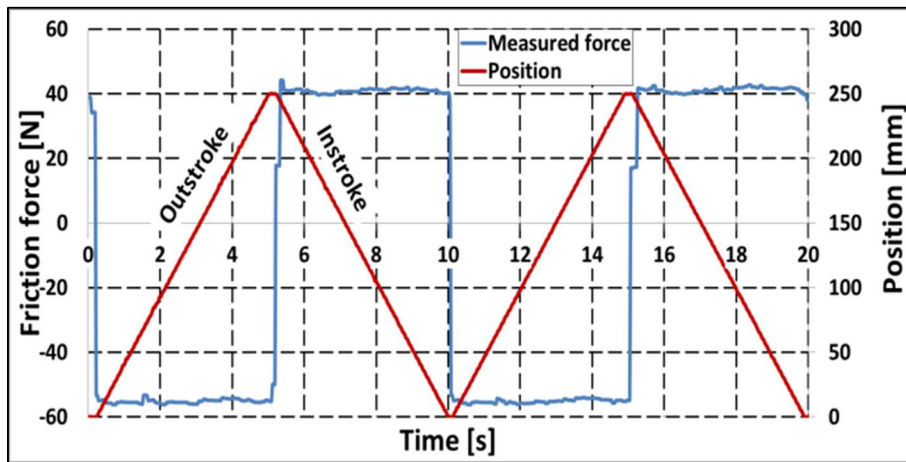


Figure 6: Friction force distribution, test 1 ($P_1=P_2=1$ bar, ± 50 mm/s)

Figure 7 shows the variation in force measured by the load sensor over four outstroke/instroke cycles at 2 bars desired pressure in chamber 2 and at a stroke speed of 50mm/s. The measured force presents a significant peak at the beginning of the stroke (whether it is instroke or outstroke). In addition, during phases of constant velocity, there are significant fluctuations in the measured force (up to 50 N in magnitude).

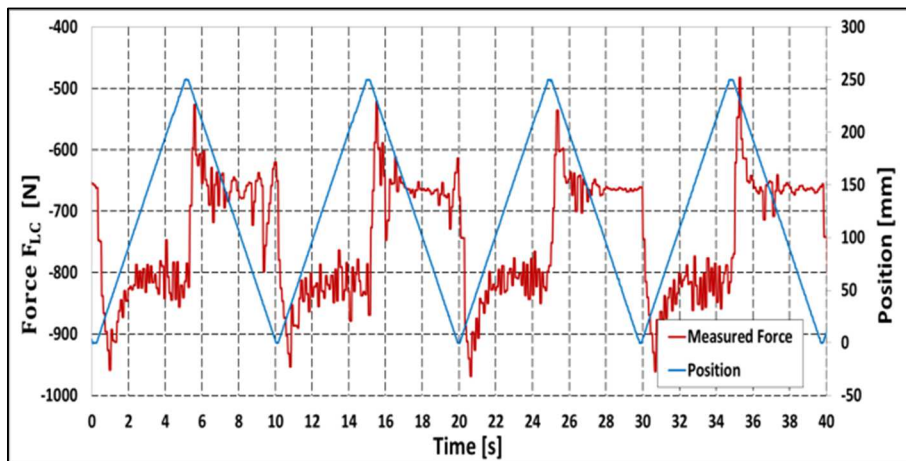


Figure 7: Measured force distribution, $P_1= 1$ bar, $P_2= 2$ bar, ± 50 mm/s

There is a very good correspondence between these fluctuations and the air pressure measured inside the chamber 2 (see Figure 8). Thus, it is concluded that the noisy aspect of the measured force is not due to any tribological phenomenon but to variations in air pressure inside the cylinder chamber. Indeed, due to the compressibility of the air and the variation in the volumes of the cylinder chamber, the used proportional valve cannot maintain a constant pressure. As a result, pressure fluctuations are recorded and their effect on the measured force is instantaneous.

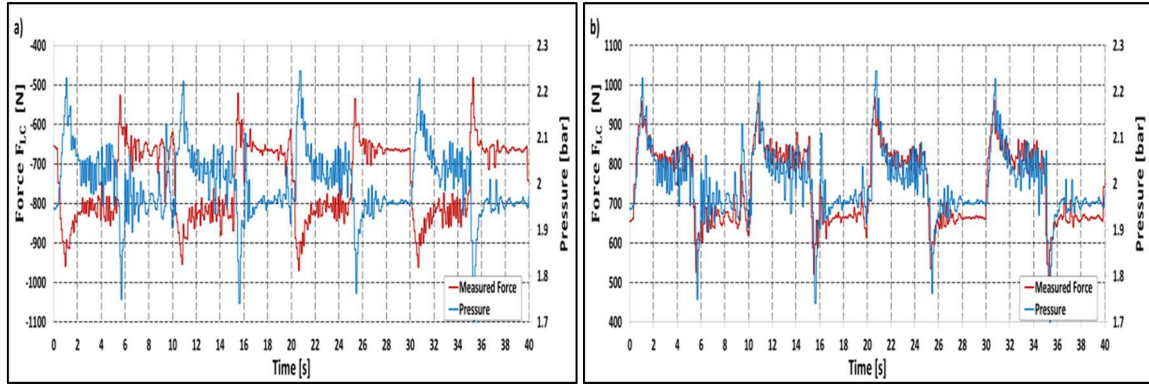


Figure 8: a) Measured force distribution, b) Absolute values of measured force distribution & Pressure distributions, $P_2=2 \text{ bar}$, $\pm 50 \text{ mm/s}$

An average friction force can be calculated according to equation 2. For different air pressure values the average friction force is shown in Figure 9 for both strokes. We note an almost linear and very important increase in friction as a function of the air pressure: passing from atmospheric to 10 bars, the friction force is multiplied by eleven.

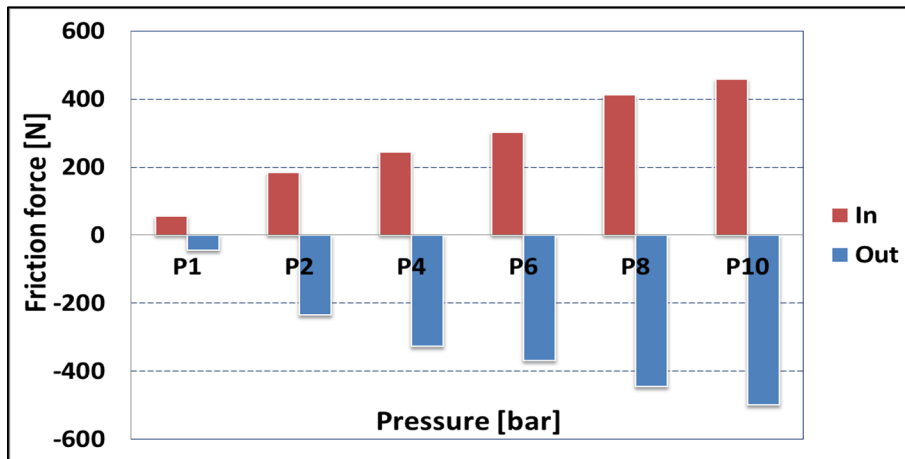


Figure 9: Average friction force versus pressure, test 1 ($P_2=1, 2, 4, 6, 8, 10$; $\pm 50 \text{ mm/s}$)

The results presented in Figure 10 are obtained for the so-called Test 2 configuration in Table 3: the two piston seals are removed from the assembly and consequently, the two cylinder chambers have the same pressure. The results are presented for the instroke and outstroke at different chamber pressures and a constant stroke speed of 50 mm/s. Since the chamber pressure can be kept constant, the variation in the friction force no longer presents the noisy pattern observed in figure 7.

As in test 1, the friction force increases with increasing pressure. It can be noted that from atmospheric to 10 bars air pressure, the friction force increases by 75% (24 N). Although this increase is significant, it is less significant than the rate of increase observed for the entire pneumatic cylinder housing (see figure 9). As also observed previously, there is an offset between the friction force values measured during the outstroke and the instroke.

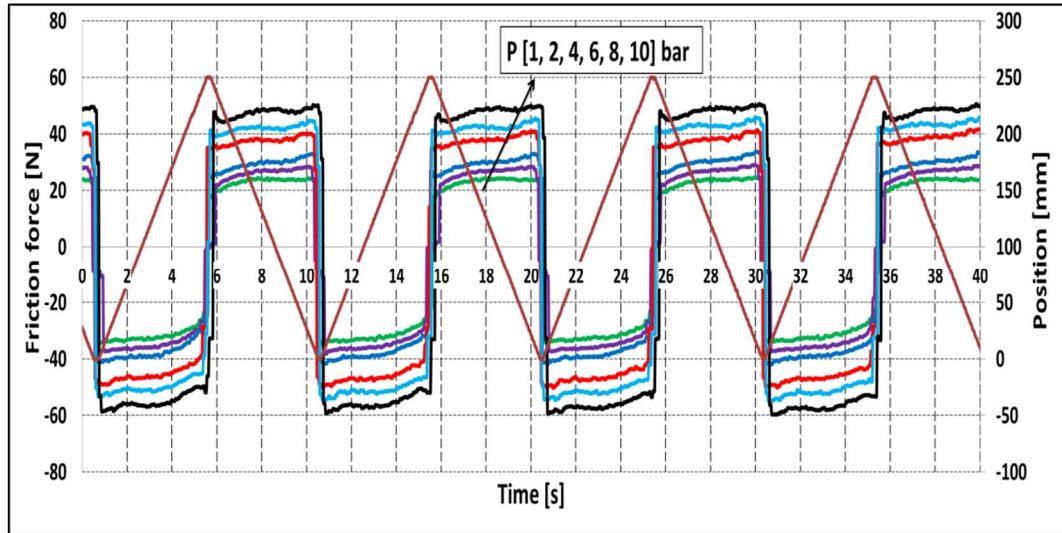


Figure 10: Friction force distributions, test 2($P_2=1, 2, 4, 6, 8, 10$; ± 50 mm/s).

The interpretation of the data presented in this section makes it possible to compare the friction generated by piston seals with that generated by the rod seals. At atmospheric pressure, the friction force of the piston seals is about 15N, which corresponds to a quarter of the total friction of the actuator. As previously indicated, when the pressure increases in chamber 2, the friction force generated by the piston seals increases more quickly than that generated by the rod seals. At 10 bars, the friction of the piston seals is about 500N, ten times the friction generated by the rod seals.

3.2. Effect of rod velocity

The experimental results shown in this section are also extracted from tests obtained on the whole cylinder configuration. Figure 11 shows the variation of the friction force for different stroke velocities and air pressures. As can be seen, regardless of the applied air pressure, the friction force increases proportionally with the velocity of the rod in both directions. In addition, there are differences in the measured force between the instroke and the outstroke: friction is lower during the instroke. Indeed, other than possible manufacturing defects of the cylinder, that have been mentioned above, when pressure is applied in chamber 2, one of the piston seals and one of the rod seals "see" the pressure when the other two seals are not pressurized. This leads to different operating conditions of the pressurized seals between the outstroke and instroke.

At atmospheric pressure, the friction force increases twice when the speed increases from 50 mm/s to 300 mm/s. This rate increases significantly with pressure: it rises to 3.4 times at 10 bars air pressure.

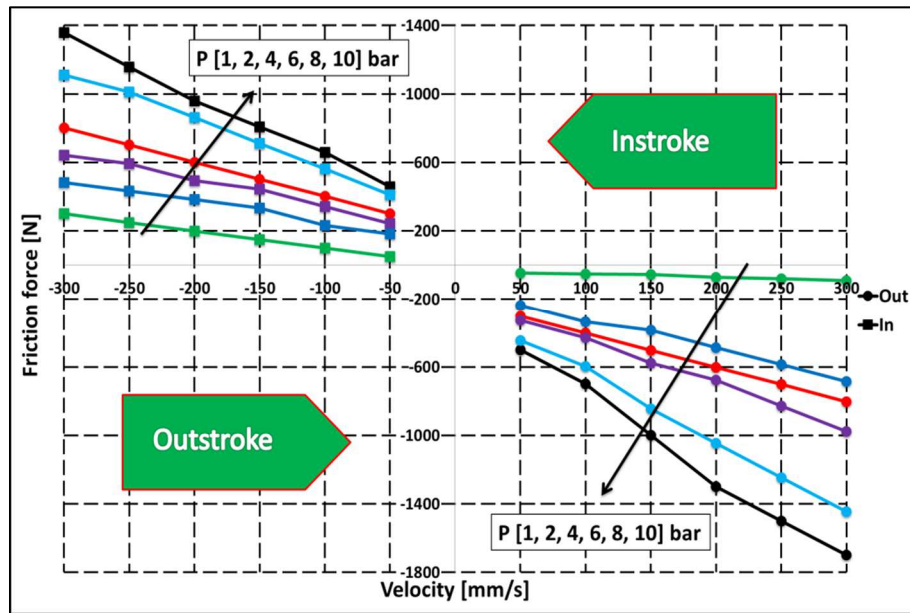


Figure 11: Friction force in function of pressure and velocity for test 1

Figure 12 shows the Pressure-Velocity (PV) diagram of absolute values of the friction force for the outstroke motion. It can be noted that the effect of pressure on the friction force is strongly influenced by the velocity and vice-versa: the higher the velocity, the greater is the increase in friction with pressure. And also, the higher the pressure, the greater is the increase in friction with speed.

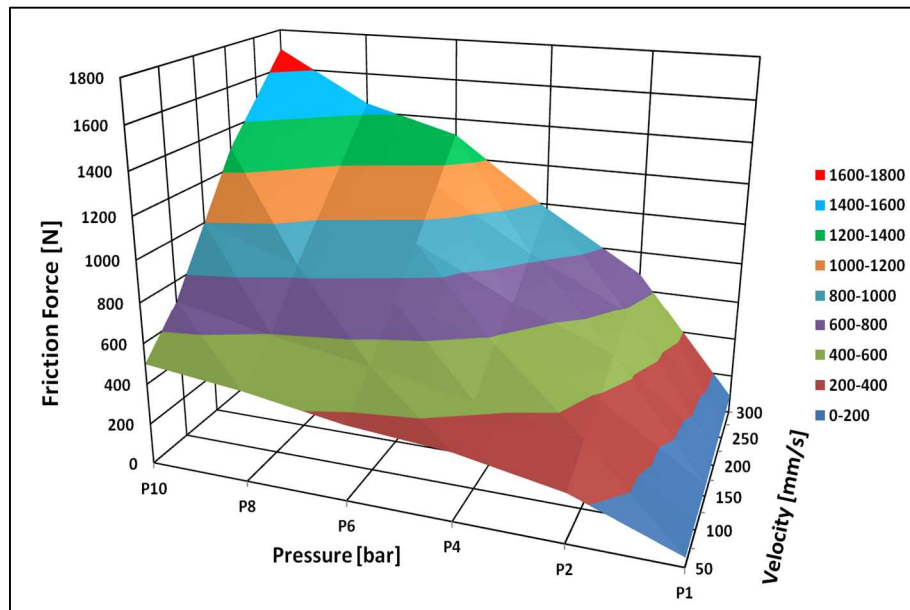


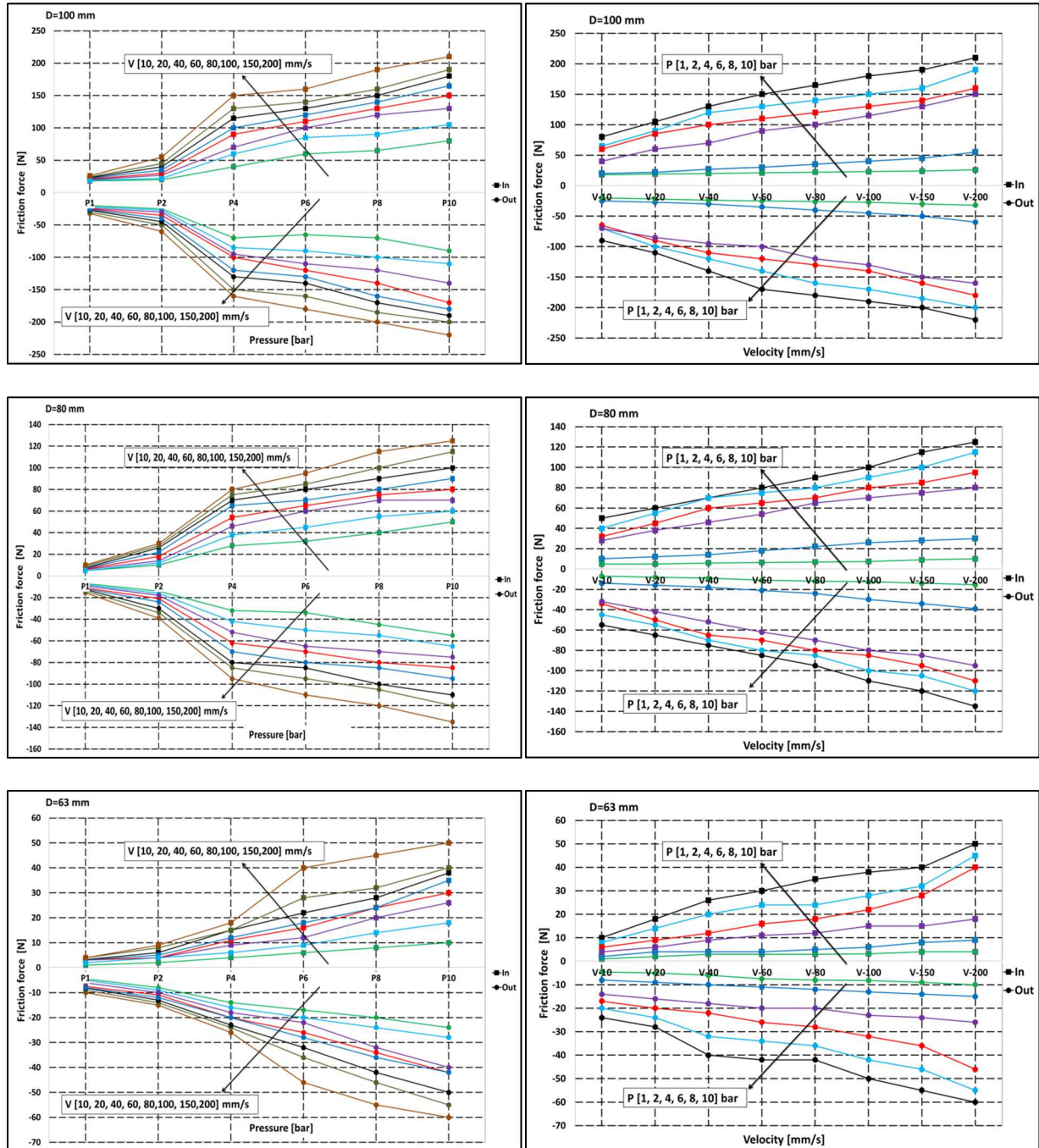
Figure 12: pressure velocity diagram

3.3. Effect of seal diameter

This paragraph concerns tests carried out to study the friction force of different piston seal geometries (configuration 2 – Tests 3 to 6 in Table 3). Figure 13, shows the average friction forces measured for the U-Cup seals with diameters ranging from 50 mm to 100 mm. It is important to mention that all the seals are made

of the same material and are supplied by the same manufacturer. The variation in friction force is presented as a function of air pressure (left-hand side in Figure 13) and velocity (right-hand side in Figure 13) and for both directions of motion.

For all the investigated diameters and both strokes, the friction force increases almost linearly with the velocity. The friction also increases with the air pressure. In all cases, except for a diameter of 63 mm, there is a relatively large increase in friction between 2 bars and 4 bars. After 4 bars, the trend is still towards an increase in the measured force but the rate of increase is less significant. For a cylinder of 63 mm in diameter, the jump noted in the friction force is observed between 4 and 6 bars.



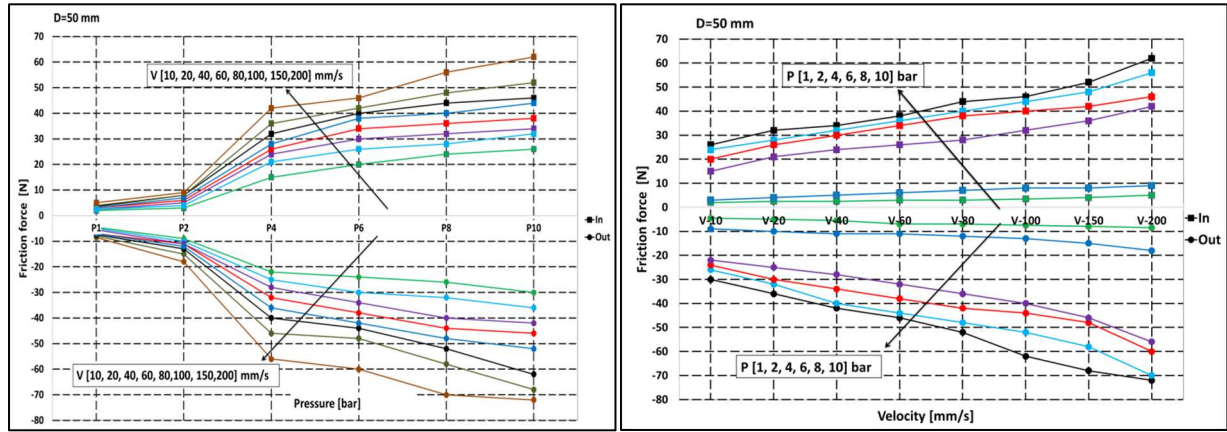


Figure 13: Friction force versus pressure and velocity for different cylinder diameter

Figure 14 shows the friction differences between the outstroke and instroke measured for all the U-Cup seals. For all the cases presented in this figure, the air pressure is set to the ambient pressure. The friction is higher during the outstroke. This can be attributed to the seal geometry that is not symmetric. However, it can be noted that the differences are quite small compared with the overall friction force and slightly increase with the velocity.

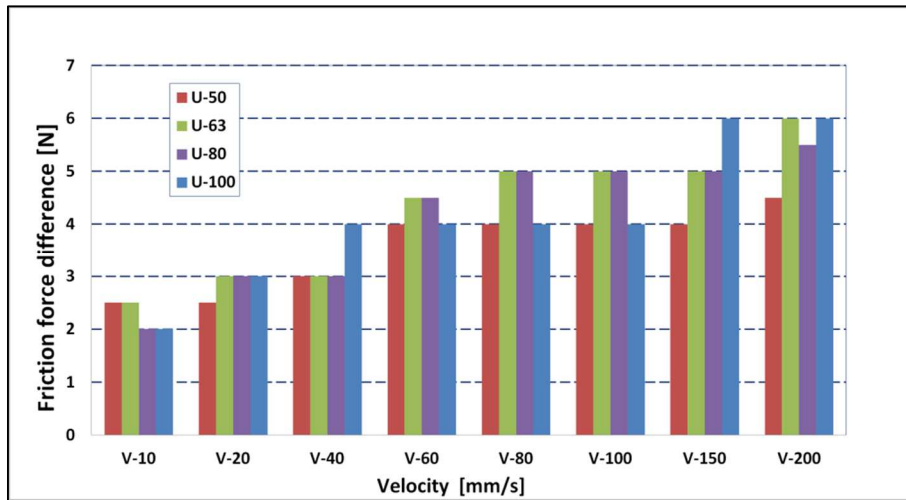


Figure 14: friction force comparison (outstroke/instroke)

Figure 15 shows the variation of the friction forces as a function of the cylinder diameter and the velocity. For all these cases the pressure is also set to the atmospheric pressure. Naturally, the friction force increases with the diameter of the cylinder but the variation is not linear: the rate of increase is higher for higher diameters. This behavior can be explained by the non-linear increase of the contact surface with the cylinder diameter.

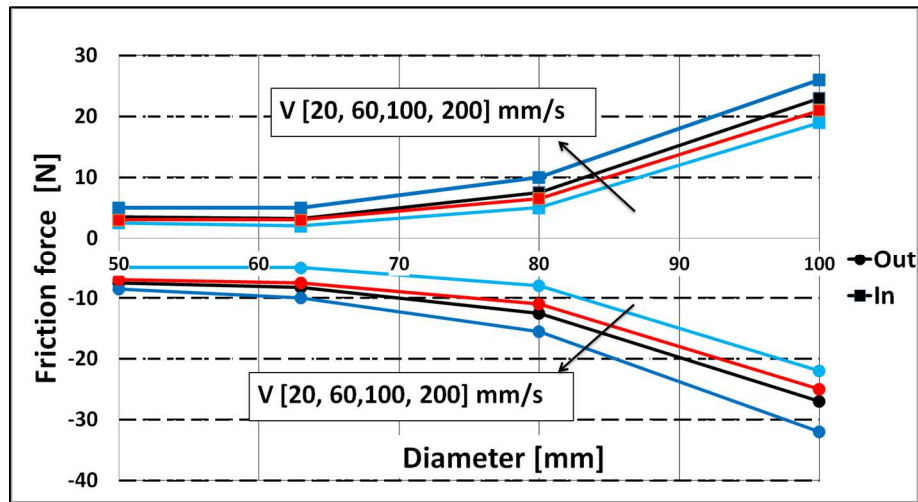


Figure 15: Friction force versus cylinder diameter

3.4. Effect of seal design

The effect of the seal design on the friction force is first investigated by comparing three piston seals of different cross-sections (U-Cup, X-Ring and O-Ring) tested separately for a cylinder diameter of 100 mm (test 3, 7 and 8 in table 3). The variation of the friction force with the air pressure and the velocity is already presented in figure 13 for the U-Cup cross-section. Figures 16 and 17 show the same results for the X-Ring and the O-Ring piston seals.

In order to better understand the differences between these three geometries, Figure 18 shows a comparison of the results obtained during the instroke at 100 mm/s and at different air pressures. It can be noted that at ambient pressure, the X-Ring seal induces the highest friction followed, in order, by the O-Ring and the U-Cup seals. All three geometries show an upward trend in friction with the chamber pressure. However, the highest rate is noted for the U-Cup seal which, for pressure levels above 2 bars, produces the highest friction. This is not surprising because the contact width between the U-Cup seal lip and the cylinder is expected to increase rapidly with the pressure. Concerning the X-Ring seal, it always shows higher friction than the O-Ring seal. Overall, for all geometries, the increase in friction for pressures above 4 bars seems to be small.

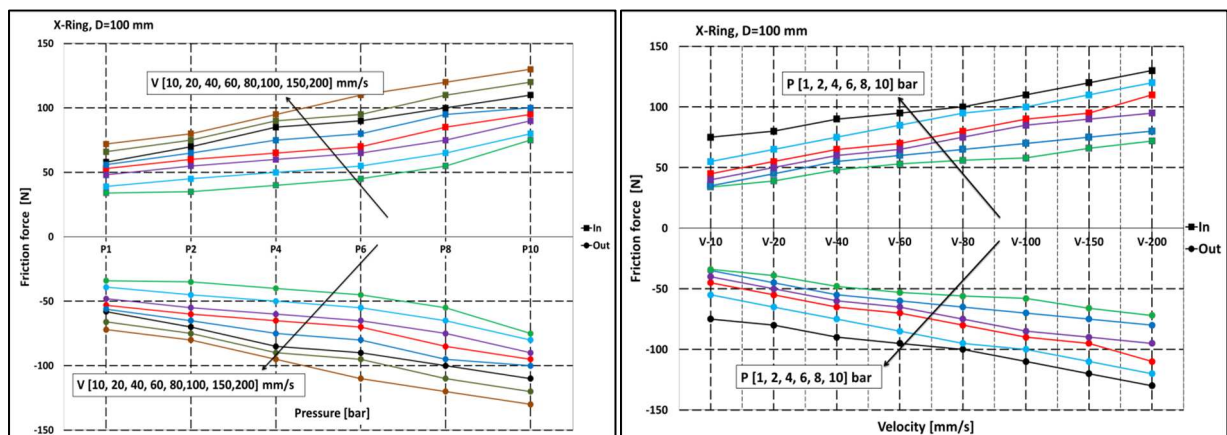


Figure 16: friction force versus pressure and velocity for X-Ring piston seal

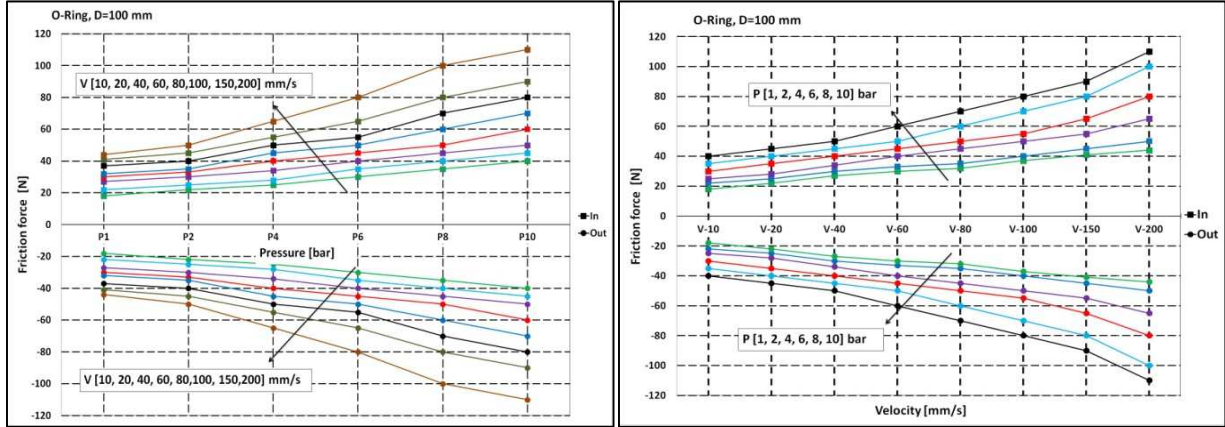


Figure 17: friction force versus pressure and velocity for O-Ring piston seal

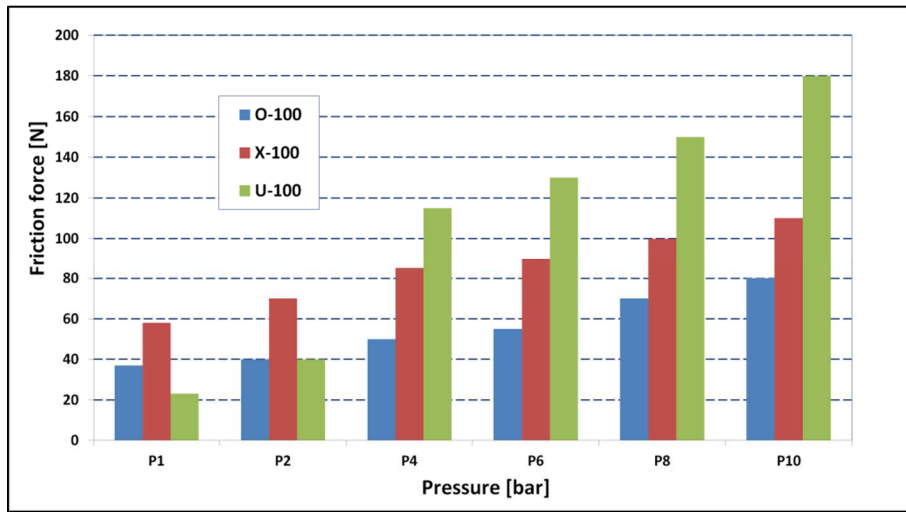


Figure 18: Comparison of friction forces during the instroke motion for three 100 mm piston seals

The effect of the seal design on the friction force is also studied for two 25 mm diameter rod seals (configuration 3 – tests 10 and 11 in table 3). Figures 19 and 20 show the variation in friction force as a function of the chamber velocity and pressure. As for the piston seals, the friction increases quasi-linear with the speed. An increase of the friction with the pressure is also observed but the linear trend is not obvious. Interesting to observe, the difference between the friction measured during the instroke and the outstroke is negligible for O-ring seals (O-25 and O-100). On the other hand, the difference is still visible for the U-25 rod seal.

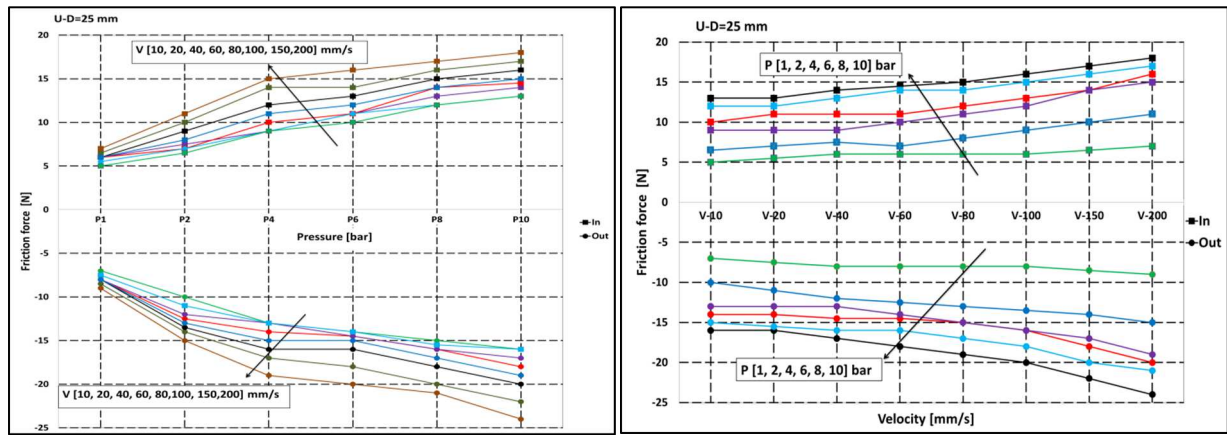


Figure 19: Friction force for a U-Cup rod seal as a function of pressure and velocity

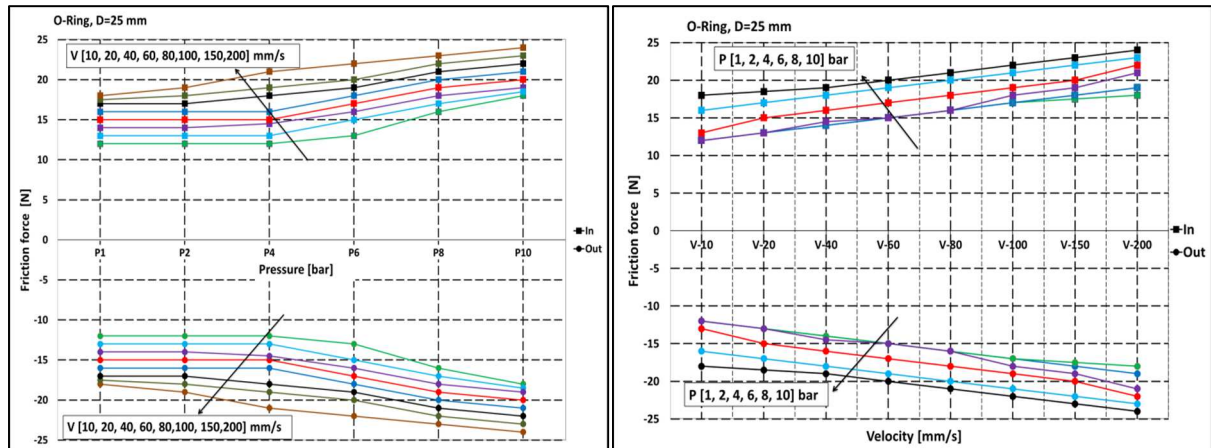


Figure 20: Friction force for an O-Ring rod seal as a function of pressure and velocity

Figure 21 shows a comparison of the results obtained for the investigated rod seals during the instroke at 100 mm/s and at different air pressures. The O-Ring seal always generates more friction than the U-Cup seal. The explanation can be found in the initial rod/seal interference that is significantly higher for the O-Ring (0.4 mm interference for the U-Cup and 1 mm for the O-Ring). However, the difference in friction between the two seals decreases with the chamber pressure.

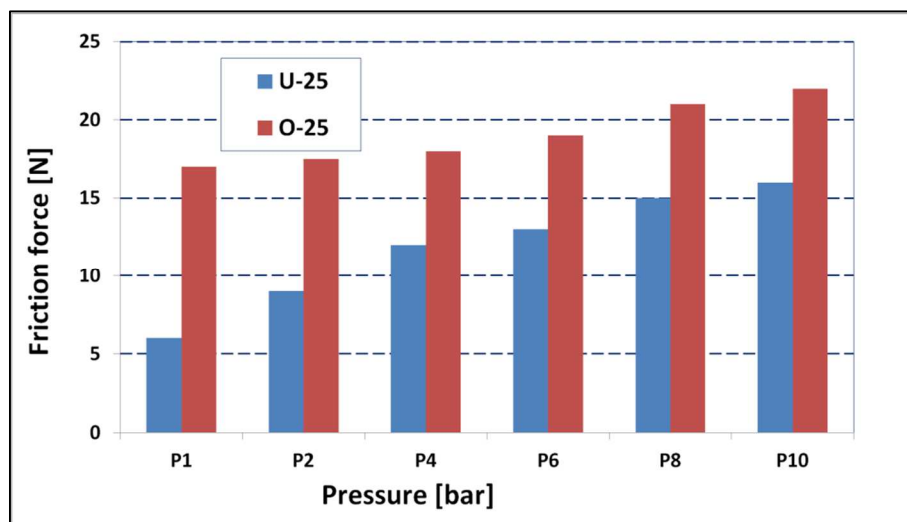


Figure 21: Comparison of friction forces during the instroke motion between U-25 and O-25 seals.

4. Dynamic friction characteristics

Figure 22 shows the variation of the friction force of a piston seal versus the rod displacement for several cycles of outstroke and instroke. The results are presented for a U-Cup seal with 100 mm of diameter functioning at 10 mm/s under atmospheric pressure.

It can be observed a slight downward trend during the outstroke and a slight upward trend during the instroke. This behavior could be explained by a small misalignment of the piston due to relatively long rod on which the piston is fixed. Also, Figure 22 shows that each stroke is preceded by a friction peak (Segment 3 in Figure 22) generated by the decrease in speed during the transition periods.

Globally, there is a good repeatability of the measured friction as, from one cycle to the next, very few differences are observed. And this is the case for the transition zones, which correspond to the change in direction of motion (segment 2 in Figure 22) but also for the steady-state zones (when the velocity is constant –segment 1 in Figure 22).

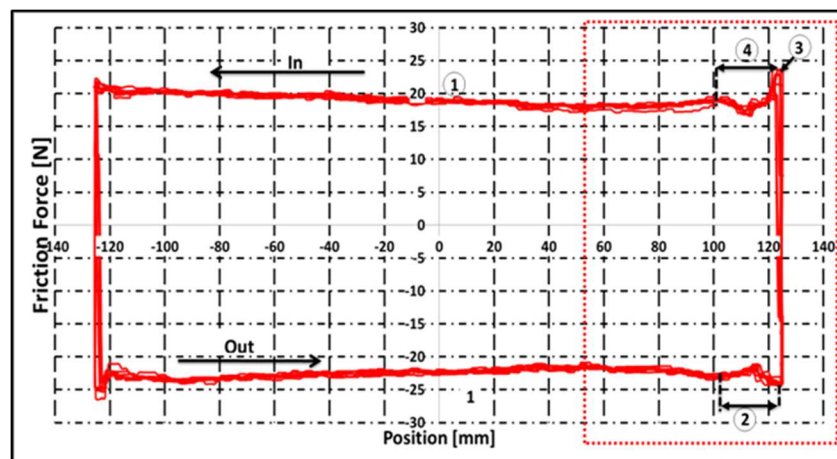


Figure 22: Friction force variation

5. Conclusions

Friction force of pneumatic seals is investigated experimentally. In this context, an experimental device has been designed and built. It allows the test of commercial pneumatic cylinders as well as the use of specific test cells designed to identify the separate behavior of rod and/or piston seals.

Experiments were performed under different operating conditions in terms of pneumatic pressures and rod velocities and for different seal designs. Results showed that for the commercial pneumatic cylinder that has been studied, at atmospheric pressure, the friction force generated by the piston seals is about 25% of the total friction force of the cylinder. This percentage increases with the air pressure: at 10 bars it is about 90% of the total friction. It has been proven that, regardless to the seal design and diameter, the friction forces increase with both air pressure and stroke velocity.

By comparing the design of the seals, it was found that the friction force generated by the U-Cup seals is more influenced by the air pressure than the O-Ring and X-Ring seals. In addition, the cross section of the seal shows a significant effect on the friction generated in the sealing area and the differences between the different seal designs increase with the increase in their diameter.

The results presented in this paper can be directly used to validate or develop theoretical models dedicated to the study of pneumatic sealing systems. In addition, the experimental set-up presented here can be used to study the influence on the friction force of other parameters, such as a lubricant, surface roughness, and seal materials.

6. Nomenclature

P_1	pressure in chamber 1	bar
P_2	pressure in chamber 2	bar
S_1	piston surface on the chamber 1 side	mm ²
S_2	piston surface on the chamber 2 side	mm ²
S_3	rod surface	mm ²
F_{lc}	load cell force (the external axial force applied on the rod)	N
F_{rs}	rod seal friction force	N
F_{rrs}	ring rod seal friction force	N
F_{ps}	piston seal friction force	N
F_{rps}	ring piston seal friction force	N
F_f	total friction force	N
m	weight of the moving part (piston, rods and seals)	Kg
γ	acceleration of the moving part	mm/s ²
V_+	positive velocity	mm/s
V_-	negative velocity	mm/s

7. References

- [01] Tokashiki L.R., Fujita T., Kagawa T., Occurrence conditions of stick-slip motion in pneumatic cylinders, driven by meter out, Proc. 6th Scandinavian Int. Conf. 2 (1999), 727-742.
- [02] Raparelli T., Bertetot A.M. Mazzat L. Experimental and numerical study of friction in an elastomeric seal for pneumatic cylinder, Tribology International, 30 (1997), No. 7, 541-552.
- [03] Belforte, G., Mattiazzo, G., Mauro, S. and Tokashiki, L.R. Measurement of friction force in pneumatic cylinders. Tribotest Journal, 2003, 10, 33-48.

- [04] Belforte, G., Conte, M., Manuello, A., & Mazza, L. (2011). Performance and behavior of seals for pneumatic spool valves. *Tribology Transactions*, 54(2), 237-246.
- [05] Ho CHANG. , Chou-Wei LAN. , Chih-Hao CHEN, Tsing-Tshih TSUNG & Jia-Bin GUO. Measurement of frictional force characteristics of pneumatic cylinders under dry and lubricated conditions, *PRZEGLAD ELEKTROTECHNICZNY* (Electrical Review), ISSN 0033-2097, R. 88 NR 7b/2012.
- [06] Belforte, G., Manuello, A., Mazza, L. Test rig for friction force measurements in pneumatic components and seals. In: *PROCEEDINGS OF THE INSTITUTION OF MECHANICAL ENGINEERS. PART J, JOURNAL OF ENGINEERING TRIBOLOGY*, vol. 227 n. 1, pp. 43-59. -ISSN 1350-6501.
- [07] G. Belforte, A. Manuello, L. Mazza: Optimization of the Cross Section of an Elastomeric Seal for Pneumatic Cylinders. *Journal of Tribology*, 128, 406-413, 2006.
- [08] C. Calvert, M. Tirovic, T. Stolarski: Design and Development of an Elastomer-Based Pneumatic Seal Using Finite Element Analysis. *Journal of Engineering Tribology*, 216 (J3), 127-138 (2002).
- [09] J. F. Archard: Contact and rubbing of flat surface. *Journal of Applied Physics*, 24 (8), 981-988, 1953.
- [10] G. Belforte, M. Velardocchia: Fault detection and dynamic behaviour of pneumatic valves. *Proceedings of IFAC Symposium on Fault Detection, Supervision and Safety for Technical Processes*, 469-474, 1994.
- [11] Mazza, L., & Belforte, G. (2017). Analytical/experimental study of the contribution of individual seals to friction force in pneumatic actuators. *Journal of Tribology*, 139(2), 022202.
- [12] G. Belforte, N. D'Alfio, T. Raparelli: Experimental analysis of friction forces in pneumatic cylinders. *The Journal of Fluid Control*, 78, 42-60, 1989.
- [13] T. Raparelli, A. Manuello, L. Mazza: Experimental and numerical study of friction in elastomeric seal for pneumatic cylinders. *Tribology International*, 30 (7), 547-552, 1997.
- [14] B. Verheyde, A. Vanhulsel, M. Rombouts, J. Meneve, D. Havermans, M. Wangenheim: Influence of surface treatment of elastomers on their frictional behaviour in sliding contact. *Wear*, doi: 10.1016/j.wear.2008.04.040.